Materials Research. 2017; 20(Suppl. 2): 167-173
DOI: http://dx.doi.org/10.1590/1980-5373-MR-2017-0077

Thermo-Mechanical Properties of P(HB-HV) Nanocomposites Reinforced by Nanodiamonds

Mariana Valinhos Barcelos[a]*, Gabriel Rodrigues de Almeida Neto[a], Fabrício Moreira Almeida[b], Rubén Jesus Sánchez Rodríguez[a], José Gregório Cabrera Gomez[c]

[a] *Laboratório de Materiais Avançados, Universidade Estadual do Norte Fluminense Darcy Ribeiro, Avenida Alberto Lamego, 2000, Parque Califórnia, Campos dos Goytacazes, RJ, Brazil*
[b] *Laboratório de Biologia do Reconhecer, Universidade Estadual do Norte Fluminense Darcy Ribeiro, Avenida Alberto Lamengo 2000, Parque Califórnia, Campos dos Goytacazes, RJ, Brazil*
[c] *Instituto de Ciências Biomédicas, Universidade de São Paulo - USP, Av. Prof. Lineu Prestes, 1374, 05508-900, São Paulo, SP, Brazil*

Received: January 17, 2017; Accepted: May 21, 2017

Several studies of biodegradable polymers and copolymers have been carried for different applications in the biomedical area. This current study aims to develop a biocomposite to be used as an orthopedic device, using poly(3-hydroxybutyrate-co-3-hydroxyvalerate) P(HB-HV), a biodegradable copolymer, with 94%HB and 6%HV, as matrix; and nanodiamonds (ND) with primary grains of 4-6nm, as reinforcement. The nanodiamonds were previously encapsulated by P(HB-HV) and specimens were prepared using a hydraulic press and injection molding machine, in order to evaluate which method presents a better performance. Thermal and mechanical analyses were done to compare their behavior. The biocomposite and pure P(HB-HV) samples were analyzed by flexural testing, nanoidentation, DMA, XRD, TGA. The distribution of nanodiamonds on the specimen fracture surface were investigated by SEM. The SEM micrographs allowed us to concluded that the encapsulation of nanodiamonds by P(HB-HV) was successfully performed, promoting a better interface and distribution in the polymeric matrix. The presence of ND in the polymeric matrix decreased the P(HB-HV) crystallinity, inhibiting the crystallite growth. The mechanical properties obtained from flexural test, nanoidentation and DMA of the injection-molded specimens were superior to compression-molded, due to its homogeneous and continuous structure. In vitro analysis was performed to evaluate the samples cytoxicity.

Keywords: *PHBV, nanodiamonds, biomaterials*

1. Introduction

Biomaterials are used to partly or totally replace the functions of a living tissue in a human body that has been damaged or traumatized[1,2]. They can be natural or artificially made[1], which in many cases combining two or more materials to form a composite.

Several studies have been done with biodegradable and biocompatible polymers and copolymers for different industries and the biomedical area. Biodegradable polymers are potential candidates to be used as biomaterials, which some possible applications are: drug-delivery vehicle, scaffolds for bone regeneration and orthopedic devices[3]. For the last application, the use of poly(L-lactic acid) (PLLA)[4], polycaprolactone (PCL)[5], P(LLA-co-CL)[6], poly(3-hydroxybutyrate) (PHB)[7] and poly(hydroxybutyrate-co-hydroxyvalerate) (P(HB-HV))[8] should be highlighted.

However, some biodegradable polymers exhibit inadequate mechanical properties for the desired application[6]. Some of the routes to solve this problem are to blend it with other polymers[9,10], synthetize copolymers[11] add plasticizers[12], or develop a composite[6].

For the development of composites, a study shows that researches regarding nano-scale materials have been increasing drastically in the last decades[13]. Different types of nanoparticles can be introduced to enhance the matrix chemical, mechanical and biological properties. Among the variety of organic and inorganic nanoparticles available, nanodiamonds (ND) presents unique properties, as high mechanical strength, biocompatibility - best among carbon-based materials, high thermal conductivity, high chemical stability and rich surface chemistry, becoming a suitable candidate to be used in biomaterials[4,14].

Few works have been reported on the addition of ND in biocompatible and biodegradable polymers. Among biocompatible polymers, Maitra et al.[15] produced composite films adding 0.2, 0.4 and 0.6 wt% of functionalized ND in poly(vinyl alcohol) (PVA) matrix; with 0.6 wt% of ND, elastic modulus (E) and hardness enhanced ~98% (1.33 GPa) and ~79% (68.4 MPa), respectively, evaluated by nanoidentation. Kurkin et al.[16] prepared composite fibers

* e-mail: marianavalinhos@yahoo.com.br

of PVA and ND, increasing ~40% of the E with only 1 v% of ND. Morimune et al.[17] prepared nanocomposite films by simple casting method of PVA/ND, in which ND content ranged from 0-5 wt%; the samples were tensile-tested, with 1 wt%, the E was 162% higher (9.6 GPa) than pure PVA. However, the strain at break reduced 43% (41%) with the same ND content. Protopapa et al.[18] dispersed ND in an autopolymerized poly(methyl methacrylate) (PMMA), from three-point bending test the E increased 76% (2.08 GPa) with ND content of 0.83 wt%. Others studies were performed for polyurethane acrylate[19] and chitosan/bacterial cellulose[20].

Regarding the biodegradable polymers, studies were restricted to PLA, PCL and its copolymers. Zhao et al.[21] fabricated nanocomposites of PLA/ND by melt compounding using an extruder and injection-molding machine. The tensile elastic modulus with 5 wt% of ND content was 19% higher than neat PLA, justified by the increment of PLA crystallinity; the authors also found the storage modulus (E') to increase for all compositions (0.1, 0.5, 1, 3, 5 wt.%). Alternatively, Zhang et al.[4] produced solution casted films with PLA and chemically functionalized ND (covalent attached octadecylamine - ODA), which promoted a fluorescent character. With 10 wt% of ND-ODA load, E and hardness increased 206% (7.9 GPa) and 820% (0.46GPa), respectively, obtained by nanoidentation. The authors also attested its biocompatibility. Later, Zhang et al.[22] published another work, where they produced PLA/ND-ODA films via solution casting followed by compression molding. The strain to failure and fracture energy increased 280 and 310%, respectively, with 10 wt% of ND-ODA. Sun et al.[6], on the other hand, prepared scaffolds using a poly(LLA-co-CL) random copolymer as the matrix adding poly-lactide functionalized ND. The authors achieved good particle dispersion and optimized mechanical properties - stiffness increased about sixfold. Fox et al.[23] produced PCL reinforced with 0.1 wt% of irradiated ND, allowing *in vitro* detection.

Most of the studies were performed on polymer thin films. Also, no work was found regarding the incorporation of ND in any polymer from polyhydroxyalkanoate (PHA) family. The present work develops a compression-molded and injection molded biocomposite with poly(3-hydroxybutyrate-co-3-hydroxyvalerate) P(HB-HV), a biodegradable polyester from the PHA family produced by microorganisms[24], reinforced by nanoparticles of diamond (ND), aiming to reach mechanical properties similar to the human bone and its bioincorporation into the bone structure.

2. Materials and Methods

2.1. Materials

In this work, both chloroform (99.8%) and ethyl alcohol (99.5%) were purchased from VETEC, Sigma Aldrich. The *Molto* diamond nanoparticles were obtained from Carbodeon Ltd Oy, with primary grains of 4-5nm. The P(HB-HV), with 6% of hydroxyvalerate content, was produced by PHB Indústria. (Mw= 52,575g/mol, Mw/Mn= 2.36. Determined by GPC in a Shimadzu LC-20AD).

2.2. Specimens preparation

To remove any impurities of the biosynthesized P(HB-HV), it went through a purification process in chloroform under reflux and precipitated in ethyl alcohol.

In an attempt to improve the dispersion of the nanoparticles in the polymeric matrix, the nanodiamonds were encapsulated by P(HB-HV). Solutions of 160mL of chloroform and 4g of purified P(HB-HV) were homogenized. Later, 0.4g of ND was added to the solution, corresponding to 10w.% Then the dispersion was evaporated, producing microcapsules, according to the methodology that is being patented. This formulation will be referred as P(HB-HV):ND(10:1).

The specimens were prepared through two different processes (injection molding and compression molding) to evaluate the influence of the molding process on the mechanical properties. The compression-molded samples were prepared as follows: 1.32g of P(HB-HV):ND microcapsules were added to the mold, being manually compacted. Then, the mold was inserted in a hydraulic press (Marcone MA 098/A) at 105ºC, aided by a lateral heating ring at the same temperature, and a compaction force of 2ton was applied. These conditions allowed the material to be molded without any apparent polymer degradation. The specimen final dimension was 35x10x3mm. The compression-molded samples will be denoted as P(HB-HV)-C and P(HB-HV):ND-C, for pure polymer and the specimens composed of P(HB-HV):ND microcapsules, respectively. For the manufacture of the injection-molded specimens, an injection molding equipment Ray-Ran RR/TSMP was used, with temperature of 174ºC at the barrel, 100ºC at the mold, and injection pressure of 6 bar. The injection-molded specimens final dimensions were: 100x13x3mm. The injection-molded specimens will be referred as P(HB-HV):ND-I.

2.3. Specimens characterization

To evaluate the influence of the ND on the thermal properties of the nanodiamonds microcapsules, Thermogravimetric analysis (TGA) was performed in TA Instruments Q5000, the samples were analyzed in a temperature range of 30-800ºC, with heating rate of 10ºC/min and nitrogen flow rate of 100mL/min.

The specimens mechanical properties were investigated by means of flexural testing, microhardness testing and dynamic mechanical analysis (DMA). In the flexural testing an universal mechanical testing machine (Instron, 5582) was used in a three-point configuration; speed of testing was set at 1mm/min, support span of 30mm. Three specimens of each formulation were tested. Nanoidentation testing was performed in an ultra-micro-hardness tester Shimadzu DUH-211S with indentation load of 30mN and Vickers

shaped diamond indenter. Seven indentations were done for each formulation; then, elastic modulus (E) was calculated. The dynamic mechanical analysis (DMA) was performed in a TA-Instruments DMA Q800 at a frequency of 1Hz, amplitude of 10 μm, using a three point bending clamp; the system was cooled to -120ºC, kept for 3min and heated at 3ºC/min until 150ºC.

The x-ray diffraction (XRD) analysis was done in a Rigaku Ultima IV equipment with Cu-Kα radiation (λ = 1.5418 Å) with a step size of 0.02º and counting time of 4s per step, 2θ ranging from 10 to 50º at 40kV accelerating voltage. The XRD was used to determine and compare the samples crystallinity. Micrographs of the samples fracture surface, obtained by a scanning electron microscope (SEM), Shimadzu SSX-550, allowed the evaluation of the nanodiamonds morphology and distribution in the material surface fracture. Then, correlate it with the previous analysis.

2.4. In vitro study

Culture of macrophages RAW 264.7 and experimentation

Murine macrophages cell lines RAW 264.7 (ATCC, TIB-71) were cultivated in a Dulbecco's Modified Medium F-12 (DMEM/ F12, Gibco BRL), supplemented with 10% fetal bovine serum (Gibco BRL) at 37ºC and 5% of CO_2, the medium was replaced every 2 days. Once the culture presented 90% of cellular confluence, the macrophages were collected for the experiments.

In the study, the macrophages were plated (4 x 10^5 cells/ well) in a 24-well plate (Costar) with 1 mL of the culture medium, specimens fragments were added to some wells. The culture was kept at 37ºC and 5% of CO_2 for 7 days. The culture medium wasn't replaced during the experimentation. In the 1st,2nd 6th and 7th testing days, 50μL of supernatant was collected from 4 different wells for the analysis of the nitric oxide (NO) production induced by the presence of the composite. Some wells were treated with 1 μg/mL of lipopolysaccharide (LPS) and their supernatants collected after 24 hours, then they were used as positive control of NO production. The collected supernatant were kept frozen at -80ºC until the moment to be analyzed.

1st and 7th day after the beginning of the test, cell viability analysis was performed using a 2% trypan-blue in a dye exclusion method, to evaluate the composites cytotoxicity. The cells were dyed with trypan-blue and analyzed using a Nikon TS100 inverted microscope, the images were captured by AxioCam (Zeiss) and manipulated with the AxionVision software (Zeiss).

2.5. Quantification of NO by Griess reaction

The quantification of NO was performed by *Griess* reaction. 50μL of the solution A (2.5mL of phosphoric acid, 0.5g of sulphanilamide, 47.5mL of milliQ H_2O) and 50 μL of the solution B (0.05g of N-1-naphthylethylenediamine, 50mL of milliQ H_2O) were mixed in a 96-well plate and incubated for 10 minutes at 37ºC. The reading was done in a microplate reader (Dynatech MR5000) using wavelength of 570nm. The standard curve was done using $NaNO_3$ concentration from 1.56μM to 200μM.

2.6. Statistical analysis

The statistical analysis was performed with one-way ANOVA and Tukey test as post test, using GraphPad Prism software (San Diego, California, USA), for the analysis of statistical significance in the experimental group defining the different error probability. Results with $p < 0.05$ were considered significant.

3. Results and Discussions

Despite numerous trials changing the processing parameters, pure P(HB-HV) couldn't be processed through injection molding, because of its limited processability, i.e. narrow range between melting and degradation temperature. The temperature required to mold it was not low enough to avoid apparent degradation.

To achieve a better ND distribution and ND-P(HB-HV) interaction, the nanofiller was encapsulated by P(HB-HV). The methodology was successful, as it is shown in Figure 1, producing regular spherical microcapsules. Thus, enabling a better dispersion of ND in the polymeric matrix, as it can be seen in Figure 2 (A-F).

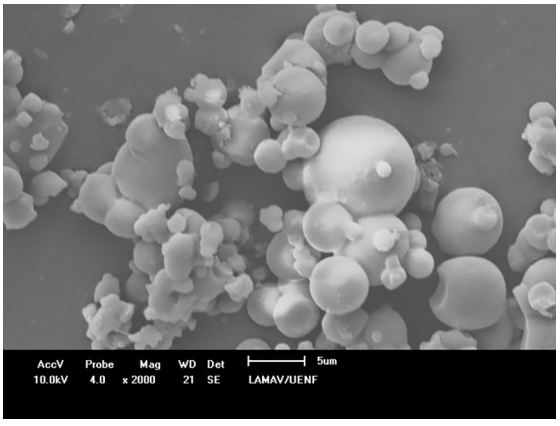

Figure 1. SEM micrograph of P(HB-HV):ND microcapsules with a magnification of 2000x.

Samples of pure P(HB-HV), pure ND and P(HB-HV):ND microcapsules were analyzed by TGA, to evaluate the influence of ND on the composites thermal behavior; the curves are presented in Figure 3, displaying the weight loss with temperature. Regarding the microcapsules, three

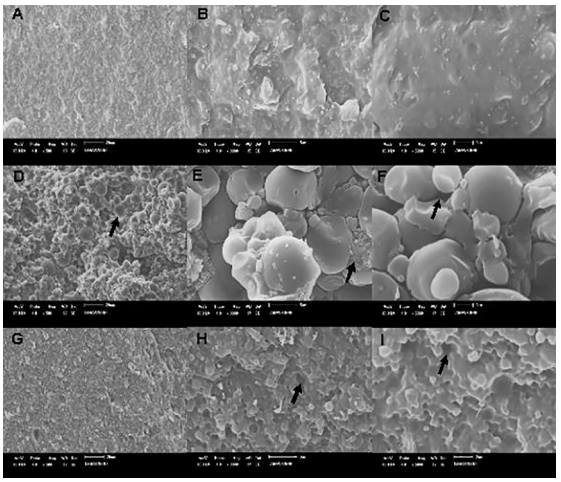

Figure 2. SEM micrographs of the specimens fracture surface, with a magnification of 500x, 3000x and 5000x, in the first, second and third column, respectively. The micrographs (A), (B) and (C) correspond to P(HB-HV):ND-I; (D), (E) and (F) correspond to P(HB-HV):ND-C; and (G), (H) and (I) correspond to P(HB-HV)-C. Voids and particles debonding are indicated by arrow.

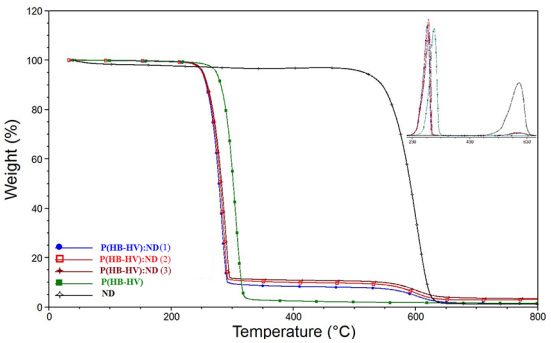

Figure 3. TGA curves of P(HB-HV)-C (filled square), P(HB-HV):ND microcapsules (filled circle, filled star, unfilled square), and ND (unfilled star).

samples from the same batch were analyzed. It is noted that for all three samples, the onset degradation temperature is 264.2ºC, which is lower than the 285.9ºC of pure polymer. It can be concluded that the introduction of ND shifts the onset temperature to lower values, justified by interaction between phases. Chen et al. observed the same trend as he added nano-hidroxyapatite (nHA) to a P(HB-12%HV) matrix. They claimed that well distributed nHA catalyzed the polymer decomposition and obstructed the degradation by-products to diffuse out of the sample[25].

TGA was also used to determine the content and distribution of ND in the microcapsules. The average content of the three samples analyzed was 7.3 ± 1.3%. Therefore, it demonstrates that a homogeneous distribution of ND was achieved. The difference between the content of ND in the solution before encapsulation (10 wt%) and present in the microcapsule is due to loss of material during the encapsulation process.

The XRD analysis (Figure 4) confirmed the semi-crystallinity of the P(HB-HV), presenting typical peaks of orthorhombic unit cell[26]. It is noted that the P(HB-HV) crystalline peaks are intensified and also shifted to lower angles after the addition of ND. The crystallinity calculated from the XRD data is 60.97 and 57.59%, for P(HB-HV) and P(HB-HV):ND, respectively. The decrease in the polymer crystallinity is justified due to the presence of ND, which obstruct the polymer chain mobility and inhibit the crystallites growth. Chen at. al[27] and Bergmann at. al[28] also found the P(HB-HV) crystallinity to decrease with filler addition. The most intense peaks, related to (002) and (110) planes, shifted to lower angles. The interplanar distance decreased from 6.63442 to 6.58215Å and from 5.29286 to 5.25136Å, of (002) and (110) planes, respectively. The addition of ND induces a less compact polymeric structure, thus increasing the interplanar distance.

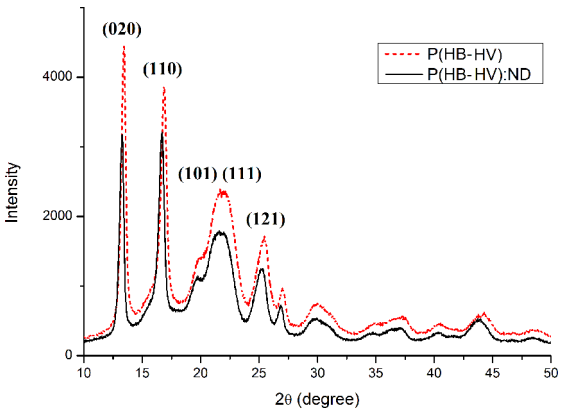

Figure 4. XRD spectra of P(HB-HV) and P(HB-HV):ND samples.

From the data obtained from flexural testing, properties like flexural elastic modulus (E), maximum flexural stress (σ_m) and maximum strain (ε) were calculated. The results are presented in Figure 5. The mechanical properties of the compression-molded specimens are inferior to the injection-molded. Justified by the presence of voids and particle debonding on the specimen fracture surface, as shown in Figure 2 (D), (E) and (F). These defects limited the potential to enhance the properties, and may even decrease it. They were originated by inexistence of polymer melting - since the molding temperature was 105ºC, which promoted a discontinuous structure.

However, for the specimens prepared by injection molding, there is an expressive increase on the mechanical properties (E, σ_m and ε) compared to the compression-molded ones. It can be justified by the continuous structure, i.e. a better polymer compaction, and homogeneous distribution of ND (Figure 2 (A), (B) and (C))), which is known for its high stiffness and hardness.

The values of elastic modulus obtained by nanoidentation are presented in Figure 6. P(HB-HV):ND-I presented superior

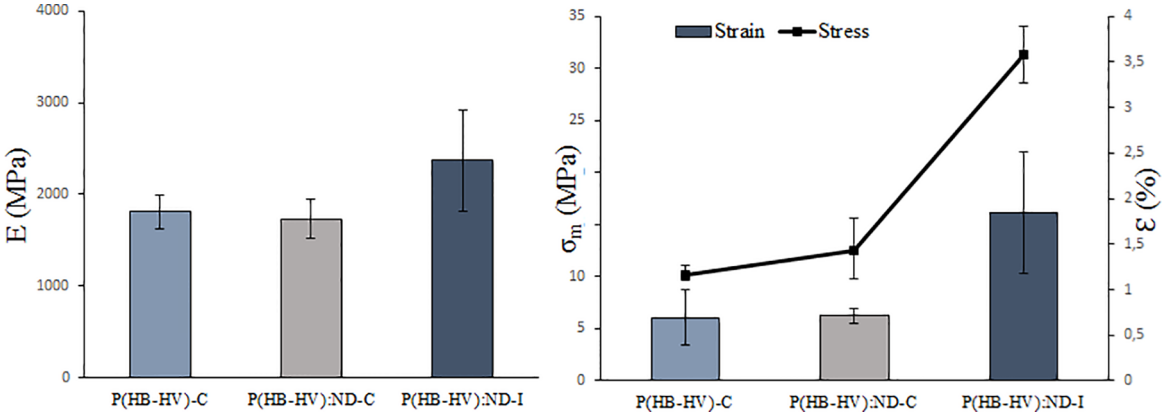

Figure 5. Mechanical Properties of different formulations obtained from three-point flexural test: Elastic modulus, maximum flexural stress and maximum strain.

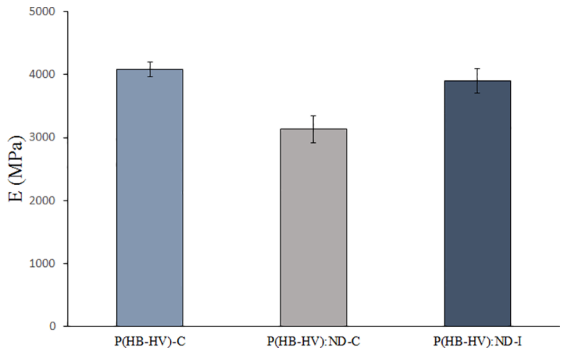

Figure 6. Elastic modulus obtained by nanoidentation of all formulations.

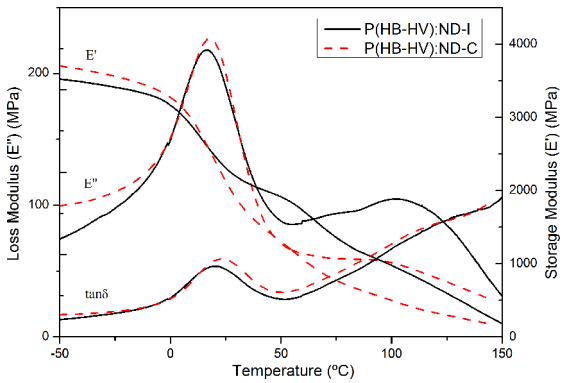

Figure 7. Storage modulus, loss modulus and tanδ variation with temperature, curves obtained by DMA for P(HB-HV):ND-I and P(HB-HV):ND-C specimens.

value than P(HB-HV):ND-C, for the same reason previously explained. However, the results for pure polymer is close to P(HB-HV):ND-I; it is believed that the stiffening mechanism of crystallinity counterpoise the ND reinforcement effect.

The DMA analysis is useful to understand the viscous and elastic contributions to the composite properties. In figure 7, it is presented the variation of storage modulus (E'), loss modulus (E'') and tanδ with temperature, of injection-molded and compression-molded specimen. It is seen that the storage modulus of P(HB-HV):ND-I is higher than P(HB-HV):ND-C at 17ºC and higher temperatures, indicating a better restriction of the polymer chain mobility, which resulted in a tougher material, for the same reason presented previously for the flexural testing. Also, the storage modulus drop is less pronounced in comparison with P(HB-HV):ND-C. The drop is related to the composites glass transition temperature.

The samples glass transition temperature (T_g) was obtained from the peak of tanδ vs temperature curves (Figure 7). The T_g of P(HB-HV):ND-I and P(HB-HV):ND-C are 20.24 and 23.25ºC, respectively. Tanδ (tanδ=E'/E''), also known as damping factor, measures the heat dissipation under cyclic loading. The P(HB-HV):ND-C displayed intenser tanδ peaks in comparison with P(HB-HV):ND-C. Intenser tanδ peaks may mean poor interface between the nanofiller and the matrix, which dissipates more energy, or a less efficient restriction of the polymeric chain mobility.

To evaluate the composite cytoxicity, the macrophages were cultivated for 7 days without replacing the culture medium. After one day of test, it was not observed any cytotoxic response, as shown in Figure 8, where there isn't cells dyed with trypan-blue. In Figure 8(C), circled in red, it is indicated viable macrophages adhered to a small P(HB-HV):ND-I specimen fragment.

After the seventh day of culture, it was observed cells dyed with trypan-blue in the control and tested cultures (Figure 9). The proportion of cells dyed with trypan-blue was similar for all cultures, regardless of the composition.

The different cultures had similar proliferation rate during the extent of the test. After the seventh day, the bottom of the plate was covered with macrophages in all culture medium. Therefore, it was concluded that the composites are non-cytotoxic and non-cytostatic.

The analysis of production of inflammatory mediator NO in the cultivated macrophages - in the presence of the composites-, concluded that until second day the cultivated macrophages didn't produce NO (Figure 10). In the sixth and seventh day, it was observed NO production in the

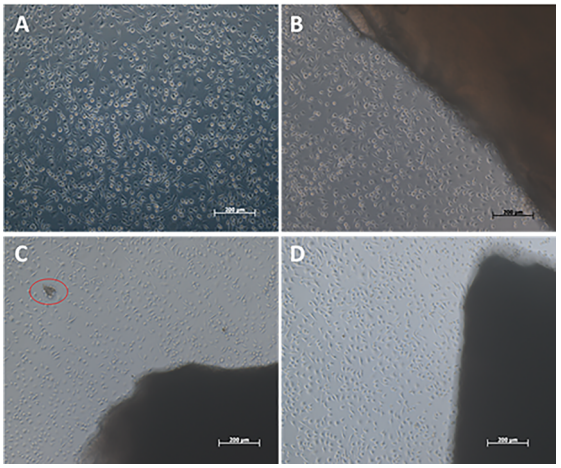

Figure 8. Macrophages cultures after the first day. The images were obtained with a magnification of 200x by an inverted microscope and corresponds to: Macrophages cultivated without the composite (A); Macrophages cultivated with the addition of pure P(HB-HV)-C specimen (B); Macrophages cultivated with the addition of P(HB-HV):ND-I specimen (C); Macrophages cultivated with the addition of P(HB-HV):ND-C (D). The red circle indicated the macrophages adhered to loose fragment from the P(HB-HV):ND-I specimen. The shadows present in the images correspond to the specimens.

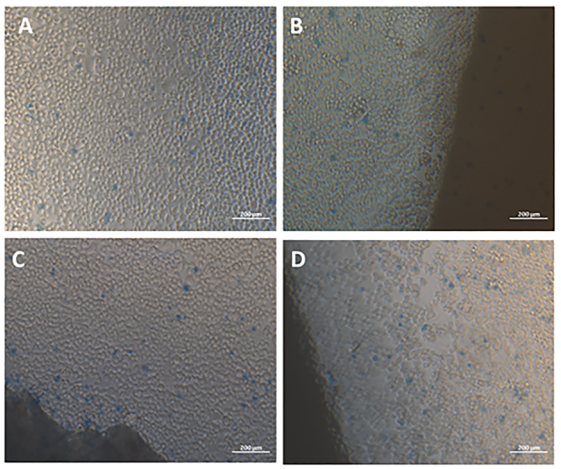

Figure 9. Macrophages culture after the seventh day. The images were obtained with magnification of 200x by an inverted microscope and corresponds to: Macrophages cultivated without the composite (A); Macrophages cultivated with the addition of pure P(HB-HV)-C specimen (B); Macrophages cultivated with the addition of P(HB-HV):ND-I specimen (C); Macrophages cultivated with the addition of P(HB-HV):ND-C (D). The dead cells are dyed blue. The shadows present in the images correspond to the specimens.

cultures where the composites were present; the production was close to 8μM, without significant difference between the formulations.

The composites triggered the NO production in the macrophages in the sixth and seventh day. This may occurred due to loose composite fragments in the well, which during the plate manipulation caused the mechanical lysis of the cells surrounding the fragment. The cell lysis could have released

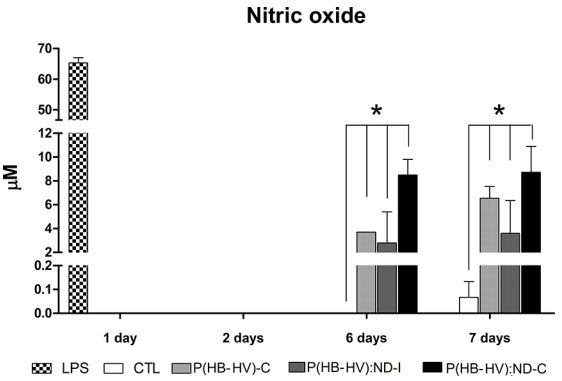

Figure 10. Production of nitric oxide by the macrophages in culture with the composites, negative (CTL) and positive control (LPS).

cells inner-substances, which stimulate the inflammatory process that accumulated with time and induced the NO production by the macrophages.

4. Conclusions

From TGA, it was concluded that the amount of ND in the sample differed from the added to the solution before encapsulation process, since there is loss of material in the encapsulation process. The injection-molded specimen presented superior flexural properties than the compression-molded, justified by a compact and homogeneous structure, promoting better distribution of load to the nanoparticles. In the compressed molded specimen fracture surface were identified, through SEM, voids and particle debonding, that weakened it. These defects may be justified by a poor compacting. The polymer crystallinity decreased with the addition of ND, due to effect of hindering the polymer chain motions. Evaluated by in vitro testing, all formulations were non-cytotoxic.

5. Acknowlwdgments

The authors would like to thank CAPES, CNPq and FAPERJ - Brazilian research agencies that supported this work.

6. References

1. Ramakrishna S, Mayer J, Wintermantel E, Leong KW. Biomedical applications of polymer-composite materials: A review. *Composites Science and Technology*. 2001;61(9):1189-1224.

2. Oréfice RL, Pereira MDM, Mansur HS. *Biomateriais: Fundamentos & Aplicações*. 1st ed. Rio de Janeiro: Guanabara Koogan; 2012.

3. Nair LS, Laurencin CT. Biodegradable polymers as biomaterials. *Progress in Polymer Science*. 2007;32(8-9):762-798.

4. Zhang Q, Mochalin VN, Neitzel I, Knoke IY, Han J, Klug CA, et al. Fluorescent PLLA-nanodiamond composites for bone tissue engineering. *Biomaterials*. 2011;32(1):87-94.

5. Oh SH, Park IK, Kim JM, Lee JH. In vitro and in vivo characteristics of PCL scaffolds with pore size gradient fabricated by a centrifugation method. *Biomaterials*. 2007;28(9):1664-1671.

6. Sun Y, Finne-Wistrand A, Waag T, Xing Z, Yassin M, Yamamoto A, et al. Reinforced Degradable Biocomposite by Homogenously Distributed Functionalized Nanodiamond Particles. *Macromolecular Materials and Engineering*. 2015;300(4):436-447.

7. Alves EGL, Rezende CMDF, Serakides R, Pereira MDM, Rosado IR. Orthopedic implant of a polyhydroxybutyrate (PHB) and hydroxyapatite composite in cats. *Journal of Feline Medicine & Surgery*. 2011;13(8):546-552.

8. Galego N, Rozsa C, Sánchez R, Fung J, Vázquez A, Santo Tomás J. Characterization and application of poly(β-hydroxyalkanoates) family as composite biomaterials. *Polymer Testing*. 2000;19(5):485-492.

9. Verhoogt H, Ramsay BA, Favis BD. Polymer blends containing poly (3-hydroxyalkanoate)s. *Polymer*. 1994;35(24):5155-5169.

10. Gupta B, Geeta, Ray AR. Preparation of poly(ε-caprolactone)/poly(ε-caprolactone-co-lactide) (PCL/PLCL) blend filament by melt spinning. *Journal of Applied Polymer Science*. 2012;123(4):1944-1950.

11. Sun Y, Finne-Wistrand A, Albertsson AC, Xing Z, Mustafa K, Hendrikson WJ, et al. Degradable amorphous scaffolds with enhanced mechanical properties and homogeneous cell distribution produced by a three-dimensional fiber deposition method. *Journal of Biomedical Materials Research - Part A*. 2012;100A(10):2739-2749.

12. Wang L, Zhu W, Wang X, Chen X, Chen G-Q, Xu K. Processability modifications of poly(3-hydroxybutyrate) by plasticizing, blending, and stabilizing. *Journal of Applied Polymer Science*. 2008;107(1):166-173.

13. Henrique PHC, Satyanarayana KG, Wypych F. Nanocomposites: synthesis, structure, properties and new application opportunities. *Materials Research*. 2009;12(1):1-39.

14. Schrand AM, Dai L, Schlager JJ, Hussain SM, Osawa E. Differential biocompatibility of carbon nanotubes and nanodiamonds. *Diamond and Related Materials*. 2007;16(12):2118-2123.

15. Maitra U, Prasad KE, Ramamurty U, Rao CNR. Mechanical properties of nanodiamond-reinforced polymer-matrix composites. *Solid State Communications*. 2009;149(39-40):1693-1697.

16. Kurkin TS, Ozerin AN, Kechek'yan AS, Gritsenko OT, Ozerina LA, Alkhanishvili GG, et al. The structure and properties of polymer composite fibers based on poly(vinyl alcohol) and nanodiamond of detonation synthesis. *Nanotechnologies in Russia*. 2010;5(5-6):340-351.

17. Morimune S, Kotera M, Nishino T, Goto K, Hata K. Poly(vinyl alcohol) Nanocomposites with Nanodiamond. *Macromolecules*. 201114;44(11):4415-4421.

18. Protopapa P, Kontonasaki E, Bikiaris D, Paraskevopoulos KM, Koidis P. Reinforcement of a PMMA resin for fixed interim prostheses with nanodiamonds. *Dental Materials Journal*. 2011;30(2):222-231.

19. Alishiri M, Shojaei A, Abdekhodaie MJ. Biodegradable polyurethane acrylate/HEMA-grafted nanodiamond composites with bone regenerative potential applications: structure, mechanical properties and biocompatibility. *RSC Advances*. 2016;6(11):8743-8755.

20. Ostadhossein F, Mahmoudi N, Morales-Cid G, Tamjid E, Navas-Martos FJ, Soriano-Cuadrado B, et al. Development of Chitosan/Bacterial Cellulose Composite Films Containing Nanodiamonds as a Potential Flexible Platform for Wound Dressing. *Materials (Basel)*. 2015;8(9):6401-6418.

21. Zhao YQ, Lau KT, Kim JK, Xu CL, Zhao DD, Li HL. Nanodiamond/poly (lactic acid) nanocomposites: Effect of nanodiamond on structure and properties of poly (lactic acid). *Composites Part B: Engineering*. 2010;41(8):646-653.

22. Zhang Q, Mochalin VN, Neitzel I, Hazeli K, Niu J, Kontsos A, et al. Mechanical properties and biomineralization of multifunctional nanodiamond-PLLA composites for bone tissue engineering. *Biomaterials*. 2012;33(20):5067-5075.

23. Fox K, Tran PA, Lau DWM, Ohshima T, Greentree AD, Gibson BC. Nanodiamond-polycaprolactone composite: A new material for tissue engineering with sub-dermal imaging capabilities. *Materials Letters*. 2016;185:185-188.

24. Chen GQ, Wu Q. The application of polyhydroxyalkanoates as tissue engineering materials. *Biomaterials*. 2005;26(33):6565-6578.

25. Chen DZ, Tang CY, Chan KC, Tsui CP, Yu PHF, Leung MCP, et al. Dynamic mechanical properties and in vitro bioactivity of PHBHV/HA nanocomposite. *Composites Science and Technology*. 2007;67(7-8):1617-1626.

26. Škrbić Z, Divjaković V. Temperature influence on changes of parameters of the unit cell of biopolymer PHB. *Polymer*. 1996;37(3):505-507.

27. Chen LJ, Wang M. Production and evaluation of biodegradable composites based on PHB-PHV copolymer. *Biomaterials*. 2002;23(13):2631-2639.

28. Bergmann A, Owen A. Hydroxyapatite as a filler for biosynthetic PHB homopolymer and P(HB-HV) copolymers. *Polymer International*. 2003;52(7):1145-1152.